On the Tangential AC Breakdown Strength of Polymer Interfaces Considering Elastic Modulus

Emre Kantar, Frank Mauseth, and Erling Ildstad
Department of Electric Power Engineering
Norwegian University of Science and Technology
Trondheim, Norway

Sverre Hvidsten
Electric Power Technology
SINTEF Energy Research
Trondheim, Norway

***Abstract*—The interfacial breakdown between two dielectric surfaces was reported to represent one of the leading causes of failure for power cable joints and connectors, in which elastic modulus of the dielectric material plays a key role. The primary motivation of this paper is to study the influence of the elastic modulus of the polymer insulation on the tangential AC breakdown strength (BDS) of polymer interfaces experimentally. In the experiments, four different materials with different elastic moduli were employed under various contact pressures: polyether ether ketone (PEEK), cured end product of epoxy resin (EPOXY), cross-linked polyethylene (XLPE), and silicone rubber (SiR). The BDS of each interface increased as the contact pressure was augmented. As the contact pressure became threefold, the interfacial BDS rose by a factor of 2.4, 1.7, 1.8, and 1.4 in the case of the PEEK, EPOXY, XLPE and SiR interface, in a sequence following the decrease of the elastic modulus. Under the same contact pressure, it was observed that the lower the elastic modulus, the higher the BDS.**

***Index Terms*—Cavity, dielectric breakdown, epoxy, partial discharge, PEEK, polymer interface, silicone rubber, surface breakdown, void, XLPE.**

I. Introduction

Subsea cable connectors are vital components of oil and gas installations, future offshore wind and wave energy systems. Although materials and production technologies for subsea applications have gained a fair amount of experience over the years, cable connectors and joints where solid-solid interfaces emerge are still considered the weaker parts of complete cable systems [1]–[3].

One of the main reasons of a solid-solid interface being weaker than its intrinsic material is that an interface contains microscopic imperfections such as cavities (see Fig. 1), protrusions, and contaminants. Such defects reduce the tangential AC electric breakdown strength (BDS) of the interface notably [1], [2]. Even in cases when the magnitude of the longitudinal electric field is much lower than the dielectric strength of the intrinsic insulation, the imperfections at the interface cause local electric field enhancements [4]. They are, thus, likely to initiate partial discharges (PD), electrical treeing, and a complete flashover might eventually follow [1]–[3].

Study of insulating materials and BDS of applications for cables and accessories has been covered to a large extent in the literature. Greenwood et al. [5] and Bhusnan [6] reported that total area of contact at an interfacial surface substantially increases in the cases when the elastic modulus is decreased, the contact pressure is augmented, or both. The interfacial breakdown between two dielectric surfaces was reported to represent one of the principal causes of failure for power cable joints and connectors, in which elastic modulus of the dielectric material plays a key role [3], [5], [6]. There is; however, still a lack of knowledge on the correlation between the elastic modulus and the BDS of the interfacial surfaces. Therefore, the primary objective of this paper is to experimentally examine the influence of the elastic modulus on the longitudinal AC breakdown strength of dry-assembled solid-solid interfaces under various contact pressures.

II. Background

When a polymer interface is assembled in dry conditions, interfacial cavities as illustrated in Fig. 1 are filled with air. The applied voltage is then distributed along strings of the cavities and contact spots. Since the dielectric strength of air is much lower than that of the polymer insulation, the dielectric breakdown will first occur in the air-filled cavities, and then the complete flashover presumably takes place eventually [2]. In the case of a homogeneous electric field, the correlation between the cavity size and the breakdown voltage (BDV) thereof is characterized by the Paschen's curve for air [7]. Referring to the left side of the Paschen's curve for air (the left branch of the V-shaped curve), it can be inferred that as the cavity length increases, the BDV of the cavity reduces.

In case of an elastic contact at the polymer interface, the interfacial cavities shrink as the contact pressure is increased, because afloat asperities come to contact and form smaller cavities with the pressure increase [5]. Sizes of the interfacial cavities changing as a function of the applied load can be determined by adopting the "deterministic contact

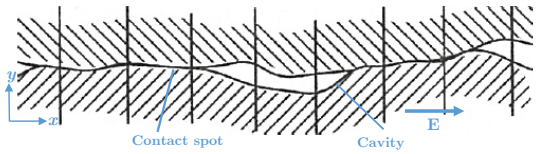

Fig. 1. An illustration of the air-filled cavities at the interface in two-dimensional profile.

The authors acknowledge the financial support of the Research Council of Norway (project no. 228344) and the SUBCONN Project Consortium.

model" addressed in [8]. The model requires a measured two-dimensional surface profile, where the interface of contact between two surfaces was governed by the theory of minimum potential complementary energy [8]. Resulting displacement of peaks and pits/valleys is then computed by minimizing an integral energy equation with respect to the applied contact pressure and material properties [8]. Only the resulting profiles of the cross-linked polyethylene (XLPE) interface are depicted in Section V to reveal the influence of the contact pressure on the cavity size quantitatively. Refer to [3], [8] for details.

III. Experimental Procedure

A. Set-up for AC Breakdown Tests

A simple illustration of the test arrangement with the dimensions of the core components is depicted in Fig. 2(a). There, two rectangular prism-shaped samples ($55\,\mathrm{mm}$ x $25\,\mathrm{mm}$ x $4\,\mathrm{mm}$) were assembled under dry ambient conditions between two Rogowski-type electrodes, forming a $4\,\mathrm{mm}$-wide interface traversed by the tangentially applied field [2].

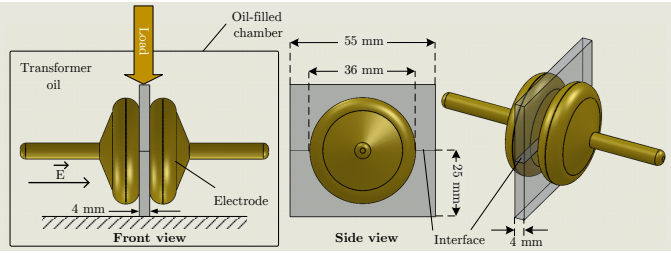

(a)

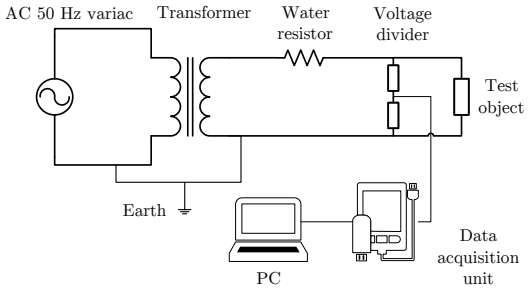

(b)

Fig. 2. (a) The simplified sketch of the mechanical test set-up. (b) The sketch of the overall electrical test set-up.

All the breakdown tests were performed with the set-up submerged in an oil-filled container to prevent any external flashover. Also, to avoid oil migration at the interface, surface pressure was applied before filling the test chamber with the oil. Fig. 2(b) shows the whole electrical test set-up. A variac ($0-230\,\mathrm{V}$, $50\,\mathrm{Hz}$) was used to energize the primary side of a $100\,\mathrm{kV}$ transformer, generating AC ramp voltage on the secondary winding at the rate of $1\,\mathrm{kV/s}$. A water resistor was employed to limit breakdown current. Moreover, a voltage divider was connected in parallel to the test object to measure the applied voltage.

B. Preparation of the Samples

The XLPE and polyether ether ketone (PEEK) samples were cut in the dimensions of $55\,\mathrm{mm}$ x $25\,\mathrm{mm}$ x $4\,\mathrm{mm}$ from a commercial, XLPE-insulated $145\,\mathrm{kV}$ power cable and VESTAKEEP 4000R smooth rod [9], respectively. In addition, we cast the epoxy and silicone rubber (SiR) in the laboratory from Casting Resin XB 5950, and Hardener XB 5951 APG [10] and Elastosil LR 3003 $-$ 60 A & B [11], respectively. The contact surfaces of the samples were polished using Struers Abramin table-top, rotating, grinding machine. As shown in [1], [2], the specimens were fixed on a steel rotating disk, and a round-SiC sandpaper of the desired grit was placed on the rotating plane. The speed of the rotating plane was set to $150\,\mathrm{rpm}$, and the force that presses the steel disk towards sandpaper was fixed to $300\,\mathrm{N}$ during polishing of all the samples, ensuring that surfaces underwent the same procedure. As a remark, SiR samples were sandwiched between XLPE samples when polishing since SiR is quite flexible and relatively soft, making a controlled contact challenging [1]. Only grit $\#500$ type sandpaper was used when polishing the surfaces since the influence of surface roughness on the tangential BDS was not studied in this work.

The samples were sanded for $2-3$ minutes with a continuous flow of water to remove any by-products and polymer remnants, and to avoid heating caused by friction. Subsequently, the samples were rinsed in tap water and were cleaned using filtered compressed air before they were washed briefly in isopropanol and were left to dry at the room temperature.

C. Elastic Modulus Measurement

The elastic modulus (Young's modulus) of each material was measured using Lloyd LR5K gauge under tensile testing. The values were determined by the initial slope of the obtained stress-strain curves following the ASTM D 790 standard. Subsequently, the effective elastic modulus E' of assembled surfaces were calculated using the following relation:

$$\frac{1}{E'} = \frac{1}{2}\left(\frac{1-{v_1}^2}{E_1} + \frac{1-{v_2}^2}{E_2}\right), \tag{1}$$

where E_1, v_1 and E_2, v_2 are the elastic modulus and Poisson's ratio of each surface, respectively [8]. The obtained results are displayed in Table I.

TABLE I
Measured Young's Modulus of Each Sample

Interface type	Young's Modulus E [MPa]	Poison's ratio v	Effective Modulus E′ [MPa]
SiR−SiR	59	0.48	109
XLPE−XLPE	200	0.46	226
EPOXY−EPOXY	4425	0.38	5166
PEEK−PEEK	7515	0.38	8808

D. Test Procedure and Data Processing

Initial interface breakdown tests were performed to identify minimum and maximum forces that the constructed set-up

permits without oil ingress and deformation of the samples, respectively. All the pressure steps determined for each interface can be found in Table II. The desired contact pressure was exerted using weights ranging between $3-75\,\mathrm{kg}$ to press the samples against one another vertically. The average contact pressure is then calculated using $p_a = F/A_a$, where F is the exerted force in N and A_a is the interface area in m^2 ($55\,\mathrm{mm}$ x $4\,\mathrm{mm}$).

For each set of experiments, eight measurements were performed using a virgin pair of samples only once. The obtained results were statistically evaluated each using the two-parameter Weibull distribution. For further evaluation, the 63.2 percentile value with the 90% confidence interval was employed.

IV. Results

The experimental data presented in Fig. 3 demonstrate that an increased elastic modulus (i.e. a harder material) results in a reduced BDS. From the minimum contact pressure ($p_{a,min} = p_{a1}$) to the maximum ($p_{a,max} = p_{a4}$), the interfacial BDS rose by a factor of $1.4-2.4$ following the increase of the elastic modulus among the chosen materials. The 63.2 percentile values for each interface are displayed in Table II. The dashed lines represent the fitted straight lines to the data points and are extrapolated in the entire pressure range in Fig. 3. The extrapolated dashed line for the SiR beyond $5.0\,\mathrm{bar}$ is higher than the tested dielectric strength of the bulk SiR ($\sim 22\,\mathrm{kV/mm}$ [11]), the line is, thus, truncated at $22\,\mathrm{kV/mm}$.

Fig. 4 was plotted to reveal the obtained correlation between the tangential AC breakdown strength and the elastic modulus. Straight lines were fitted to the data points and were extrapolated within the entire modulus range. Filled markers represent the experimentally obtained values while the hollow marker stands for the extrapolated data extracted from Fig. 3.

The impact of the contact pressure on the cavity structure is illustrated in Fig. 5 on a two-dimensional surface texture profile obtained from a virgin XLPE sample polished by #500 grit sandpaper. There, two surfaces, one rough and one nominally flat (horizontal zero-axis) are assembled, and the rough surface is pushed towards the flat surface. As seen, afloat asperities come to contact with the flat surface, and the area of contact expands as the pressure is augmented from $5.0\,\mathrm{bar}$ to $33.4\,\mathrm{bar}$. The predicted maximum cavity; thus, shrinks from $115\,\mu\mathrm{m}$ to $23\,\mu\mathrm{m}$. The largest cavities at the given contact pressure were determined by applying the deterministic contact model in [8] as stated in Section II. The selected estimated cavity sizes in relation to the applied pressure and the elastic modulus are depicted in Table III.

V. Discussion

The results presented in Fig. 3 and Table II indicated that the rate of change in the BDS from $p_{a,min}$ to $p_{a,max}$ culminates when $E' = 8808$ MPa (PEEK-PEEK); whereas, the lowest gradient is encountered in the case of $E' = 109$ MPa (SiR-SiR). However, the ratio of $p_{a,max}/p_{a,min}$ in the case of SiR-SiR is not as high as those in the other cases. Because

TABLE II
Overview of the Experimental Results

Interfacial pressure	SiR-SiR		XLPE-XLPE		EPOXY-EPOXY		PEEK-PEEK	
	p_a [bar]	63.2% [kV/mm]	p_a [bar]	63.2% [kV/mm]	p_a [bar]	63.2% [kV/mm]	p_a [bar]	63.2% [kV/mm]
p_{a1}	**1.6**	10.0	**5.0**	7.0	**11.6**	8.9	**11.6**	6.3
p_{a2}	**1.9**	12.1	**8.6**	9.6	**16.7**	10.0	**16.7**	8.1
p_{a3}	**2.4**	14.3	**11.6**	10.3	**22.5**	12.6	**22.5**	11.1
p_{a4}	**2.7**	14.5	**16.7**	12.8	**33.4**	15.6	**33.4**	15.1

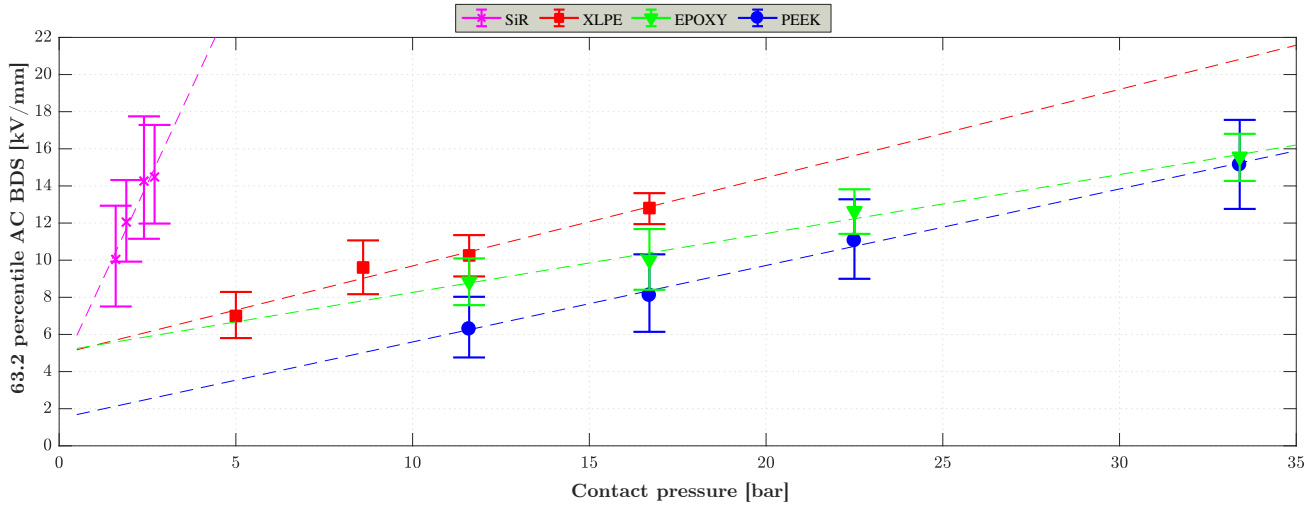

Fig. 3. The 63.2 percentile BDS with the 90% confidence intervals vs. the contact pressure. The vertical bars feature the 90% confidence interval of the 63.2 percentile for each case; whereas, the markers point the 63.2 percentile. The dashed lines represent the fitted straight lines to the data points.

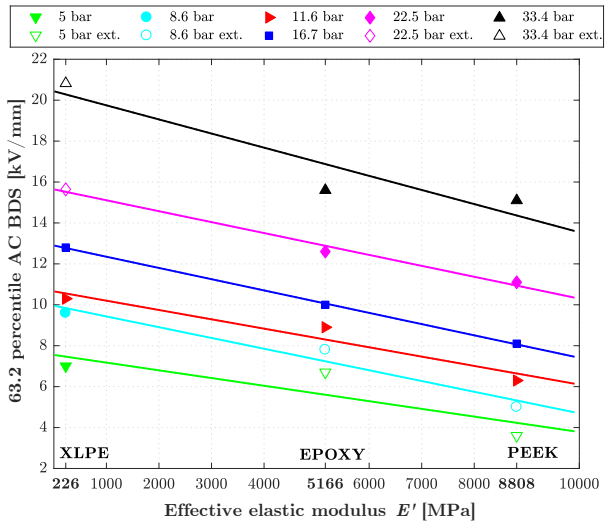

Fig. 4. The 63.2 percentile BDS as a function of the effective elastic modulus. (ext: extrapolated data using Fig. 3.)

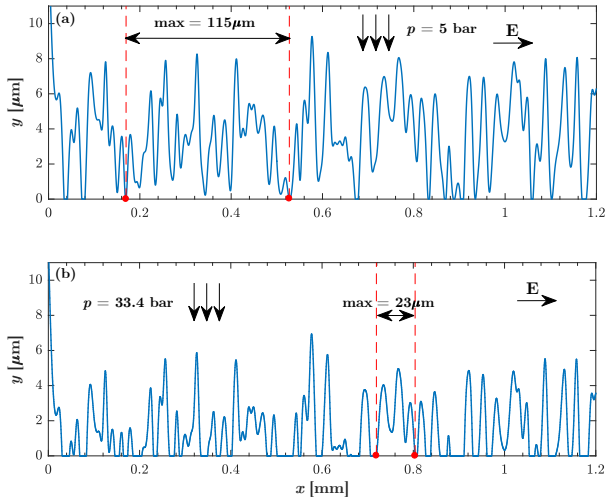

Fig. 5. The displacement of peaks and dips on the measured XLPE surface profile under: (a) 5.0 bar. (b) 33.4 bar. ($xy-$plane w.r.t. Fig. 1.)

it was implausible to reduce $p_{a,min}$ further to prevent oil ingress while $p_{a,max}$ could not have been increased due to substantial deformation of the samples. Nevertheless, it can still be inferred that the elastic modulus of the material plays an important role in the interfacial BDS as follows. In Fig. 3, the 63.2 percentile BDS of the EPOXY and PEEK interfaces can compare with that of the SiR interface only at contact pressures at least ten times as high. It is interesting to observe that materials with low modulus such as the SiR can achieve such high BDS values even at low contact pressures.

Similar to the respective influence of the contact pressure on the BDS, the elastic modulus affects the size of cavities. When the modulus is lower, increasing the contact pressure can push the asperity tips further than it does in the case of higher elastic modulus [1]–[3], [5]. That, in turn, yields smaller cavities as shown in Fig. 5, and hence a higher BDS in accordance with the Paschen's law [3].

As depicted in Table III, although the maximum cavity sizes

TABLE III
ESTIMATED LENGTH OF THE LARGEST CAVITIES

Interfacial cavity[1]	5.0 bar	11.6 bar	16.7 bar	33.4 bar
XLPE [μm]	115	71	51	23
EPOXY [μm]	168	96	62	42
PEEK [μm]	236	150	114	61

[1] The estimated cavity sizes of the SiR: $88 - 65\,\mu$m from $1.6 - 2.7$ bar, respectively.

are not much comparable under pressures as low as 5.0 bar, the difference tends to become much less prominent as the applied contact pressure is increased. Therefore, having cavities of comparable size is likely to yield similar BDS values despite the difference in elasticity of interfaces. For instance, the BDS values at the same contact pressure in Fig. 3 becomes almost indiscernible beyond 20 bar particularly in the case of the EPOXY and PEEK interfaces, indicating that increase in modulus renders the average cavity sizes comparable at the same contact pressure.

VI. Conclusion

The experimental results indicated that the lower the elastic modulus, the higher the BDS. The employed deterministic model predicted smaller cavities as the elastic modulus is reduced, suggesting increased interfacial BDS values that agree with the experimental results. Besides, the interfacial BDS rises up with the increased contact pressure in all cases independently on the elastic modulus. To be able to correlate the interfacial BDS with the elastic modulus in a clearer way, further experiments on the PD inception voltages of the cavities are essential and are intended as the future work.

References

[1] E. Kantar and E. Ildstad, "Modeling longitudinal breakdown strength of solid-solid interfaces using contact theory," in *2016 IEEE Int. Conf. on Dielec. (ICD)*, vol. 1, July 2016, pp. 398–401.

[2] E. Kantar, S. Hvidsten, F. Mauseth, and E. Ildstad, "Longitudinal AC breakdown voltage of XLPE-XLPE interfaces considering surface roughness and pressure," *IEEE Trans. Dielectr. Electr. Insul.*, vol. 24, no. 5, 2017.

[3] S. M. Hasheminezhad, "Tangential electric breakdown strength and PD inception voltage of solid-solid interface," Ph.D. dissertation, Norwegian University of Science and Technology, 2016.

[4] E. Kantar, S. Hvidsten, F. Mauseth, and E. Ildstad, "Tangential AC breakdown strength of solid-solid interfaces considering surface roughness," in *IEEE Conf. Electr. Insul. and Dielectr. Phen. (CEIDP)*, 2017.

[5] J. Greenwood and J. Williamson, "Contact of nominally flat surfaces," in *Proc. Royal Society of London A: Mathematical, physical and engineering sciences*, vol. 295, no. 1442, 1966, pp. 300–319.

[6] B. Bhushan, "Analysis of the real area of contact between a polymeric magnetic medium and a rigid surface," *Journal of Tribology*, vol. 106, no. 1, pp. 26–34, 1984.

[7] L. A. Dissado and J. C. Fothergill, *Electrical degradation and breakdown in polymers*. IET, 1992, vol. 9.

[8] A. Almqvist, "On the effects of surface roughness in lubrication," Ph.D. dissertation, Luleå tekniska universitet, 2006.

[9] "PI-VESTAKEEP-4000G-EN data sheet," Evonik Industries AG, Essen, Germany.

[10] "Casting Resin XB 5950 / Hardener XB 5951 APG data sheet," Huntsman Int. LLC, The Woodlands, Texas.

[11] "ELASTOSIL LR 3003/60 A/B data sheet," Wacker Chemie AG, Munich, Germany.